



## Antithrombotic, Antihemolytic Activities and Protein Conjugation Properties of Silver Nanoparticles Synthesized from *Turbinaria ornata*

AMALAN VENKATESAN<sup>1,\*</sup>, JOSE VINOTH RAJA ANTONY SAMY<sup>1,\*</sup>, RAJESWARI RANGA ANANTHA SAYANAM<sup>2,\*</sup>,  
JAYAPRAKASH RAJENDRAN<sup>3,\*</sup> and VIJAYAKUMAR NATESAN<sup>1,\*</sup>

<sup>1</sup>Department of Biochemistry and Biotechnology, Faculty of Science, Annamalai University, Chidambaram-608002, India

<sup>2</sup>Department of Biochemistry, Vinayaka Mission's Kirupananda Variyar Medical College and Hospitals, Vinayaka Mission's Research Foundation (Deemed to be University), Salem-636308, India

<sup>3</sup>Department of Chemistry, School of Arts and Science, Aarupadai Veedu Campus, Vinayaka Mission's Research Foundation-Deemed to be University, Paiyanur-603104, India

\*Corresponding author: E-mail: [nvkbiochem@yahoo.co.in](mailto:nvkbiochem@yahoo.co.in)

Received: 26 March 2021;

Accepted: 24 April 2021;

Published online: 26 July 2021;

AJC-20421

Green synthesis of silver nanoparticles synthesized from *Turbinaria ornata* weed extract was carried out. Because these seaweeds are largely unexplored and contain botanical molecules that promote bimolecular reduction. In this study, silver nanoparticles (AgNPs) cause a rise in the accumulation of clotting factors, platelets and procoagulant activity, both of which lead to thrombotic and hemolytic diseases. The silver nanoparticles were initially characterized using spectroscopic analysis to validate the biomolecules of *Turbinaria ornata* involved in nanoparticle reduction. A detailed study on the effectiveness of silver nanoparticles on antithrombotic activity in adult blood samples confirms the interaction of nanoparticles with platelets and blood vessels, which is significant in the production of thrombosis and cardiovascular diseases. The antihemolytic activity was tested to assess the percentage of blood clot lysis in order to confirm the ability to scavenge hydrogen peroxide in a concentration dependent manner. The protein conjugation and binding activities of major, secondary, and tertiary structures were also investigated *in silico*. Thus, *Turbinaria ornata* seaweeds with reduced silver nanoparticles demonstrated increased antithrombotic and antihemolytic activities, suggested that they could be used as novel therapeutics for cardiovascular diseases.

**Keywords:** Silver nanoparticles, Antithrombotic, Antihemolytic, *Turbinaria ornata*, Bioreduction.

### INTRODUCTION

Recent prevalence of thrombolytic and hemolytic diseases, as well as the rising mortality rates in recent years, has spurred research into medication lead targeted discovery. In the treatment of cardiovascular disorders, the drug conjugated targeted nanotechnology-based delivery system offers in-site action as therapeutics. The production of natural plant-based nanoparticles has demonstrated a wide range of increased reaction with minimal to no side effects [1]. The recent interest in green nanoparticle synthesis has grown in importance, with reports of increased anti-platelet, antihemolytic and anti-aggregation action. Algae are a class of chlorophyll-containing, oxygen consuming, photosynthetic organisms that are genetically diverse and present in a number of marine environments [2].

Microalgae are unicellular microscopic (m) species that can occur naturally or in populations, including commercially important *Chlorella vulgaris* and *Dunaliella salina*. Macroalgae, also known as seaweed, are large multicellular organisms that normally inhabit coastal waters, while green macroalgae can be found in freshwater ecosystems [3]. Seaweeds are plant-like plants that live in coastal areas on rock or other hard substrate. *Turbinaria ornata* is a tropical brown alga of the fucale's order that is found only on South Pacific coral reefs. They will soon colonies these ecosystems, thanks in part to their system of dispersal, which consists of detaching older and more buoyant fronds that float on surface currents, mostly in large rafts with many individual thalli or fronds [4]. Fucoxanthin, a xanthophyll pigment, predominates in these algae, giving them their brown colour. Brown algae (Phaeophyceae) are a type of *Turbinaria* that grows on rocky substrates in tropical marine waters. *Turbinaria*

*ornata* has been shown to have low levels of phenolics and tannins [5,6].

Silver nanoparticles (AgNPs) have emerged as a key product in nanotechnology. The AgNPs activities have a benevolent impact on all facets of human life [7]. Silver nanoparticles have been extensively used in the production of medicinal drugs due to their advantages such as decreased size and stability, selective activity, biocompatibility, sustained release action, and minimized toxicity and side effects [8-10].

*in vitro* Hemolytic activities are emerging as a new area of drug lead discovery research. Researchers are looking at ethnobotanically important plants in order to discover new natural products with anti-inflammatory properties [11]. These results are important because some patients have developed addiction to conventional treatments, such as aspirin and/or opioid drugs, and have been diagnosed with medicinal plants. This causes a major issue for society. However, the excessive use of illegal drugs poses serious threat to civilization [12,13]. Erythrocytes, the most diverse cells in the human body with appealing physiological and morphological characteristics, are widely used in drug delivery. The oxidative degradation of the erythrocyte membrane (lipid/protein) has been linked to hemolysis in other hemoglobinopathies [14], toxic medications, metal transfer overload, radiation and deficits of certain erythrocyte antioxidant systems [15]. Traditional medicine systems are popular in developed countries, where upto 80% of the population depends on traditional medicines or folk remedies for primary health care [16].

As a result, the present study focuses on the *in vitro* experimental study of antithrombotic and antihemolytic responses. Furthermore, bioinformatics analyses were carried out in order to identify the proteins responsible for the therapeutic action demonstrated by the formulated AgNPs prepared by green synthesis of *Turbinaria ornata* seaweed extract.

## EXPERIMENTAL

Silver nitrate (Merck, India), other chemicals and all the microbiological media were obtained from HiMedia Lab., India. Ultrapure MilliQ water was used throughout the study.

Human blood was collected of five healthful individuals, with showed  $25\text{ }^{\circ}\text{C} \pm 10$  years of age to evaluate *in vitro* assays. The study was conducted in accordance with approval by Human Ethic Committee of Vinayaka Mission's Kirupananda Variyar Medical College and Hospitals and the consent was obtained for all the five subjects.

**Collection of *Turbinaria ornata* seaweeds:** *Turbinaria ornata* used in the study was collected randomly from the region of in around marine Biotechnology, Parangipet, India and authenticated. *Turbinaria ornata* was dried in air, made in to a fine powder and stored in an air tight bottle. The aqueous extracts were then, dried in vacuum and stored in a refrigerator. Whole algal powder (60 g) yielded 10.2 g of crude extract.

**Synthesis of silver nanoparticles:** For the synthesis of AgNPs, 50 mL of *Turbinaria ornata* extract was heated to 60-80 °C with a mechanical stirrer with hot plate. Silver nitrate (5 g) was added to the solution when the temperature attained 60 °C.

This mixture was then heated until it turned into a dark brown suspension. This sample was centrifuged at 6000 rpm for 30 min. A soft brown colored powder was gathered at the bottom and carefully separated, dried and stored [17,18].

**Characterization:** The characteristic peaks of the synthesized silver nanoparticles were studied using ultraviolet and FT-IR spectral analysis [19]. Spectral analysis using ultraviolet spectroscopy validated the synthesis and bioreduction of the produced AgNPs. The formulated suspension was observed at routine intervals of time, and the maximal absorption was scanned between 300nm and 600nm. Further, the spectrum scan data were analyzed. The interaction between the bonding molecules of silver nanoparticles reduced from *Turbinaria ornata* and the presence of biomolecules responsible for reduction were studied using Fourier Transform Infrared spectral analysis. The spectral data were obtained from the dried extraction mixture, which recorded peaks. The observed peaks were interpreted further to validate the bio reduction of silver nanoparticles from *Turbinaria ornata* seaweeds.

**Antithrombotic activity:** Good donor's venous blood was collected and placed in sterile pre-weighed micro centrifuge tubes (0.5 mL/tube) and incubated at 37 °C for 45 min. Following clot forming, serum was fully drained without disrupting the clot and each clot was measured again to determine the clot's weight. Test drug (100 µL) was applied separately to each micro centrifuge tube containing pre-weighed clot. Streptokinase (100 µL) and filtered water (100 µL) were applied separately to control tubes I and II as a normal and a non-thrombolytic control, respectively. Both tubes were then incubated at 37 °C for 90 min and visually examined for clot lysis. During incubation, the fluid was drained and the tubes were weighed again to calculate the weight difference after clot death. The difference in weight obtained before and after clot lysis was calculated as a percentage of clot lysis. The experiment was replicated with blood samples from the remaining five patients [20,21].

**Antihemolytic assay:** Blood was drawn from healthy adult human donors, stored in sterile tubes and used within 5 h. In a set of test tubes, diluted 800 µL of 1% w/v Triton X-100 to a volume of 3 mL with sterile phosphate buffer, while 3 mL of distilled water served as a positive control. Various concentrations of plant extracts (100-500 g) were added to a series of tubes which had previously been incubated with Triton X-100. RBC suspension (500 µL) was gently mixed into each tube before being incubated at 37 °C for 1 h and centrifuged for 5 min. To approximate the percentage of hemolysis, the absorbance of the supernatant was measured at 541 nm against the phosphate buffer as a blank [22].

**in-silico Protein analysis:** Genbank database hosted by the NCBI was used to retrieve the FASTA sequences of the proteins. ExPasy ProtParam (<http://us.expasy.org/tools/protparam.html>) was used to compute the primary structure prediction. Secondary structure prediction was computed using self optimized prediction method with alignment (SOPMA). The characterization was obtained by SOSUI and TMHMM v.2.0 tools were used to characterize the proteins whether it exists in soluble or transmembrane in nature. InterPro is a comprehensive database of protein families, domains and functional sites. Tertiary

structure prediction was obtained by homology simulation using a fully automatic protein structure modelling server. The swiss model and the structure was visualised and analyzed using the visualisation programme Rasmol. InterPro combines the most important protein signature databases into a single resource. InterPro protein sequencing and classification predicted super-family and the molecular structure.

Protein sequence alignment was carried out using the pair wise sequence alignment tool (NCBI-BLAST) (<http://blast.ncbi.nlm.nih.gov/Blast.cgi>) and multiple sequence alignment was done using the EBI-CLUSTAL OMEGA (<http://www.ebi.ac.uk/Tools/msa/clustalo/>) tool. Clustal Omega has also important features for connecting sequences and exploiting information in current alignments, using the large amount of precomputed information available in public databases such as Pfam. Protein phylogenetic studies were carried out to determine the number of proteins that share similar structural and functional characteristics. All sequences in FASTA formats were fed into Clustal Omega with default options. The bootstrap Neighbour Joining (NJ) approach was used to construct the phylogenetic tree. Bootstrap analysis of 1000 replicates was used to test the stability of the internal nodes. The performance was evaluated for fully matched sequences, ratings, orientation, conserved residues, replacements and semi-conserved substituted residue patterns [23].

**Statistical analysis:** The biochemical parameters studied were subjected to statistical analysis using Sigma Stat Statistical Package (Version 3.1). The experimental results were expressed as mean  $\pm$  SD.

## RESULTS AND DISCUSSION

**UV-Visible studies:** The UV-Vis spectrum of dispersed AgNPs absorbed radiations at approximately 382 nm (Fig. 1). Significant peak in *Turbinaria ornata* extracts with colourless silver nitrate indicate the formulation of AgNPs. AgNPs had band gap energies of 3.692 eV, which correspond to the characteristic absorption peak of AgNPs [24]. The study found major peaks, which are consistent with the other results [25].

**FT-IR studies:** The FT-IR spectrum of *Turbinaria ornata* extracts with colloidal AgNPs suggests that different functional groups are arranged molecularly. Peaks observed at different

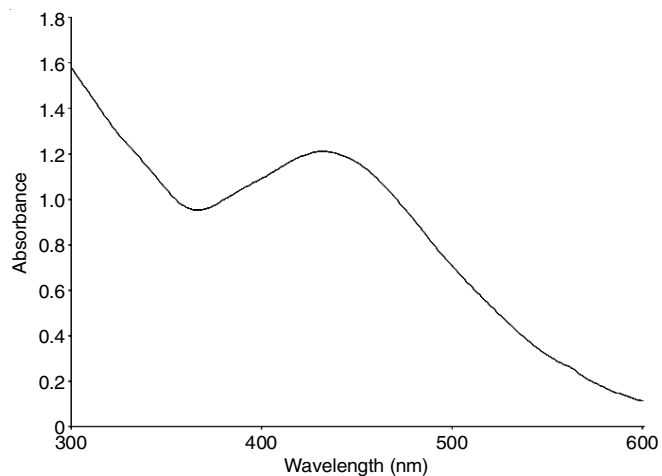


Fig. 1. UV-vis absorption spectra of *Turbinaria ornata* with 1 mM AgNO<sub>3</sub>

absorption bands at 4307, 3390, 2825, 871, 439 and 420 cm<sup>-1</sup>, which are characteristic of -OH stretching vibration and -CH stretching vibration. The peak at 871 cm<sup>-1</sup> could be due to the asymmetrical and symmetrical stretching vibrations metal conjugated carboxylates, resulting in carboxylic group involvement in proteins [26]. The bending and stretching vibrations confirmed that -OH stretching around 3390 cm<sup>-1</sup> and -CH stretching around 2825 cm<sup>-1</sup> are responsible for the heavy capping on the AgNPs nanoparticles (Fig. 2).

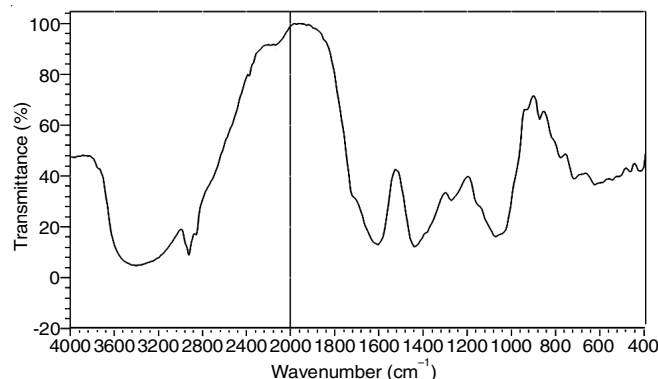


Fig. 2. FT-IR spectra of AgNPs synthesized using *Turbinaria ornata* extract

### *in-vitro* Antithrombotic activity of AgNPs of *Turbinaria*

**ornata:** The antithrombotic activity of AgNPs synthesized from *turbinaria ornata* demonstrates the antithrombotic agents with improved efficacy for preventing or treating arterial or venous thrombosis. Increased activation of plasminogen by fibrin-dependent and fibrin-independent mechanisms, similar to streptokinase, causes extra production of plasmin, which breaks down fibrin, the main constituent of thrombi, to dissolve unwanted blood clots [22].

Table-1 interprets that the antithrombosis activity of *T. ornata* synthesized AgNPs was monitored through the lysis of blood clot as observed 71% and the values were compared with normal streptokinase 81% (Fig. 3). The synthesized AgNPs was found to have substantial antithrombolytic activity, close to the reported article [27], and the extract was at least partially related to its ability to inhibit platelet aggregation.

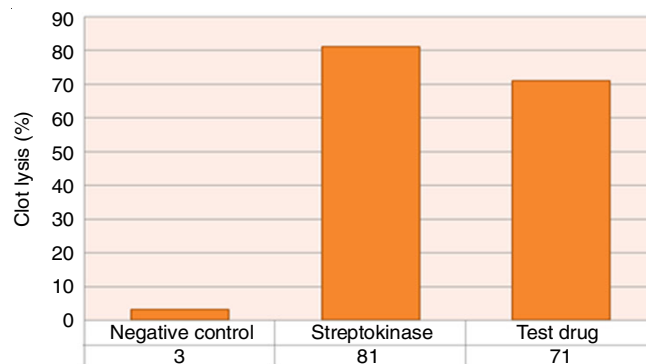


Fig. 3. Percentage of clot lysis vs. streptokinase standard vs. test drug

**Antihemolytic activity:** Table-2 shows that the synthesized AgNPs from *T. ornata* extract indicated the extreme activity against hemoglobin induced linoleic acid pathway due

TABLE-1  
in vitro ANTITHROMBOTIC ACTIVITY OF AgNPs OF *Turbinaria ornata*

| Weight of empty tubes | Weight of tube with clot | Weight of clot | Weight of tube with clot after lysis | Weight of lysis | % of clot lysis | Average % of clot lysis |
|-----------------------|--------------------------|----------------|--------------------------------------|-----------------|-----------------|-------------------------|
| A (g)                 | B (g)                    | C = (B-A) (g)  | D (g)                                | E = (B-D) (g)   |                 |                         |
| 0.081                 | 1.431                    | 0.350          | 1.179                                | 0.252           | 72              |                         |
| 1.064                 | 1.512                    | 0.448          | 1.202                                | 0.310           | 69              |                         |
| 1.077                 | 1.491                    | 0.414          | 1.184                                | 0.307           | 74              | 71                      |
| 1.089                 | 1.453                    | 0.364          | 1.209                                | 0.244           | 67              |                         |
| 1.072                 | 1.478                    | 0.406          | 1.181                                | 0.297           | 73              |                         |

% of clot lyses = (wt. of released clot/clot weight) × 100

TABLE-2  
EVALUATION OF ANTIHEMOLYSIS  
OF AgNPs - *Turbinaria ornata*

| Concentration of plant extract (µg/mL) | Antihemolytic activity (%) |
|--|----------------------------|
| 100                                    | 69                         |
| 80                                     | 53                         |
| 60                                     | 36                         |
| 40                                     | 25                         |
| 20                                     | 16                         |

to the presence of a high total phenolic contents in the extract, acting as a potential antihemolytic medication [28]. In general, the extract showed satisfactory antihemolytic activity as a percentage of inhibiting activity, ranging from 16 to 69% and the IC<sub>50</sub> was 74 µg/mL.

The enhanced properties of the synthesized AgNPs from *Turbinaria ornata* could scavenge H<sub>2</sub>O<sub>2</sub> in a concentration-dependent manner. Theoretically, synthesized AgNPs from *Turbinaria ornata* regulate the oxidation of unsaturated fatty acids. A decrease in the concentration of polyunsaturated fatty acids (PUFA) in the membrane and oxygen transfer coupled with redox active haemoglobin molecules causes erythrocytes to be attacked by free radicals. Lipid peroxidation is caused by the formation of singlet oxygen and hydroxyl radicals by superoxide anion [29].

**in silico Analysis of proteins in *Turbinaria ornata*:** The protparam method was used to predict the primary structure (Table-3). Expasy's protparam method was used to compute the parameters, which showed that the molecular weights for ten distinct proteins were 73385.66 (NADH). Ubiquinone oxidoreductase this amino acid sequence is a part of a membrane protein which has 16 transmembrane helices, 48050.97 (RBCL: this amino acid sequence is of a membrane protein which have

2 transmembrane helices), 27368.12 (ATP synthase subunit: this amino acid sequence is of a membrane protein, which have 14 transmembrane helices), 54533.22 (PsaA: this amino acid sequence is of a membrane protein, which have 5 transmembrane helices), 15433.56 (ribosomal protein L16), 22384.69 (elongation factor), 30414.34 (secy-independent protein translocation), 22751.52 (NADH-dehydrogenase subunit 11), 4857.93 (uncharacterized protein: this amino acid sequence is of a membrane protein which have 1 transmembrane helix), 47581.84 (cytochrome B: this amino acid sequence is of a membrane protein, which have 9 transmembrane helices). The pI of four proteins was less than 7 suggested that they are acidic and the pI of six proteins was greater than 7 indicated that they are simple in nature. At their pI, the proteins are found to be small and stable. Eight of the ten proteins have an instability index less than 40, which means that they are stable [30,31].

The aliphatic proteins index was determined to be between 85.00 and 140.52. Extinction coefficients computed in this analysis assist in the quantitative study of protein-protein and protein-ligand interactions in solution. The GRAVY (Grand Average of Hydropathicity) range of *T. ornate* proteins was discovered to be between -0.018 and -0.561. The lowest GRAVY value suggests the probability of stronger water contact [32].

SOPMA was used to predict the secondary structure of *Turbinaria ornata* proteins (Table-4), which showed that α-helix, extended chain, β-transform and random coil were more normal. The α-helix dominates all ten proteins, followed by the random coil, extended chain and β-flip. The secondary structure was projected with the default parameters, which were window width: 17, resemblance threshold: 8 and number of states: 4. TMHMM v.2.0 and SOSUI believed that the soluble proteins remaining four proteins were transmembrane proteins (Table-5).

TABLE-3  
EXPASY PROTOPARAM PROTEINS OF *Turbinaria ornata*

| Protein                                | Accession number | Length | m.w.     | PI    | -R | +R | EC     | II    | AI     | GRAVY  |
|--|------------------|--------|----------|-------|----|----|--------|-------|--------|--------|
| NADH-ubiquinone oxidoreductase         | A0A0G2RKW7       | 661    | 73385.66 | 7.10  | 33 | 33 | 120180 | 35.86 | 113.30 | 0.871  |
| RBCL                                   | A0A022NV54       | 438    | 48050.97 | 5.58  | 51 | 42 | 68300  | 26.63 | 89.11  | -0.019 |
| ATP-Synthase subunit                   | A0A0G2RLB2       | 249    | 27368.12 | 6.26  | 7  | 5  | 28670  | 32.19 | 140.52 | 1.338  |
| PsaA                                   | A1X1X6           | 491    | 54533.22 | 6.80  | 28 | 24 | 103945 | 26.75 | 101.96 | 0.313  |
| Ribosomal protein L16                  | A0A0G2RKU9       | 137    | 15433.56 | 10.80 | 7  | 32 | 9970   | 25.20 | 96.20  | -0.561 |
| Elongation factor TU                   | QQQCE5           | 205    | 22384.69 | 4.52  | 35 | 20 | 9970   | 24.66 | 110.20 | -0.018 |
| Secy-independent protein translocation | A0A0G2RL73       | 258    | 30414.34 | 9.44  | 10 | 22 | 41050  | 30.35 | 116.40 | 0.581  |
| NADH-dehydrogenase                     | A0A0G2RLB7       | 204    | 22751.52 | 8.22  | 18 | 21 | 21720  | 40.39 | 85.00  | 0.091  |
| Uncharacterized protein                | A0A0G2RKV3       | 41     | 4857.93  | 10.66 | 2  | 8  | -      | 16.39 | 95.12  | 0.390  |
| Cytochrome-b                           | A0A0G2RL24       | 418    | 47581.84 | 8.87  | 20 | 25 | 117355 | 42.00 | 103.54 | 0.539  |



| TABLE-4<br>SECONDARY STRUCTURE OF PROTEINS OF <i>Turbinaria ornata</i> |             |            |            |        |            |        |            |            |            |            |
|--|-------------|------------|------------|--------|------------|--------|------------|------------|------------|------------|
| Secondary sutures  | Proteins    |            |            |        |            |        |            |            |            |            |
|  | A0A0G2RKKW7 | A0A22ONV54 | A0A0G2RLB2 | A1X1X6 | A0A0G2RKU4 | Q0QCE5 | A0A0G2RL73 | A0A0G2RLB7 | A0A0G2RKY3 | A0A0G2RL24 |
| Alpha helix  | 51.29       | 45.21      | 51.81      | 44.60  | 20.44      | 34.15  | 55.04      | 14.71      | 73.17      | 45.45      |
| Extended strand  | 21.03       | 13.01      | 18.07      | 17.72  | 25.55      | 21.95  | 16.28      | 28.43      | 7.32       | 16.99      |
| Beta turn  | 4.69        | 4.57       | 4.82       | 5.50   | 8.76       | 7.80   | 2033       | 9.80       | 0.00       | 4.07       |
| Random coil  | 23.00       | 37.21      | 25.30      | 32.18  | 45.26      | 36.10  | 26.36      | 47.06      | 19.51      | 33.49      |

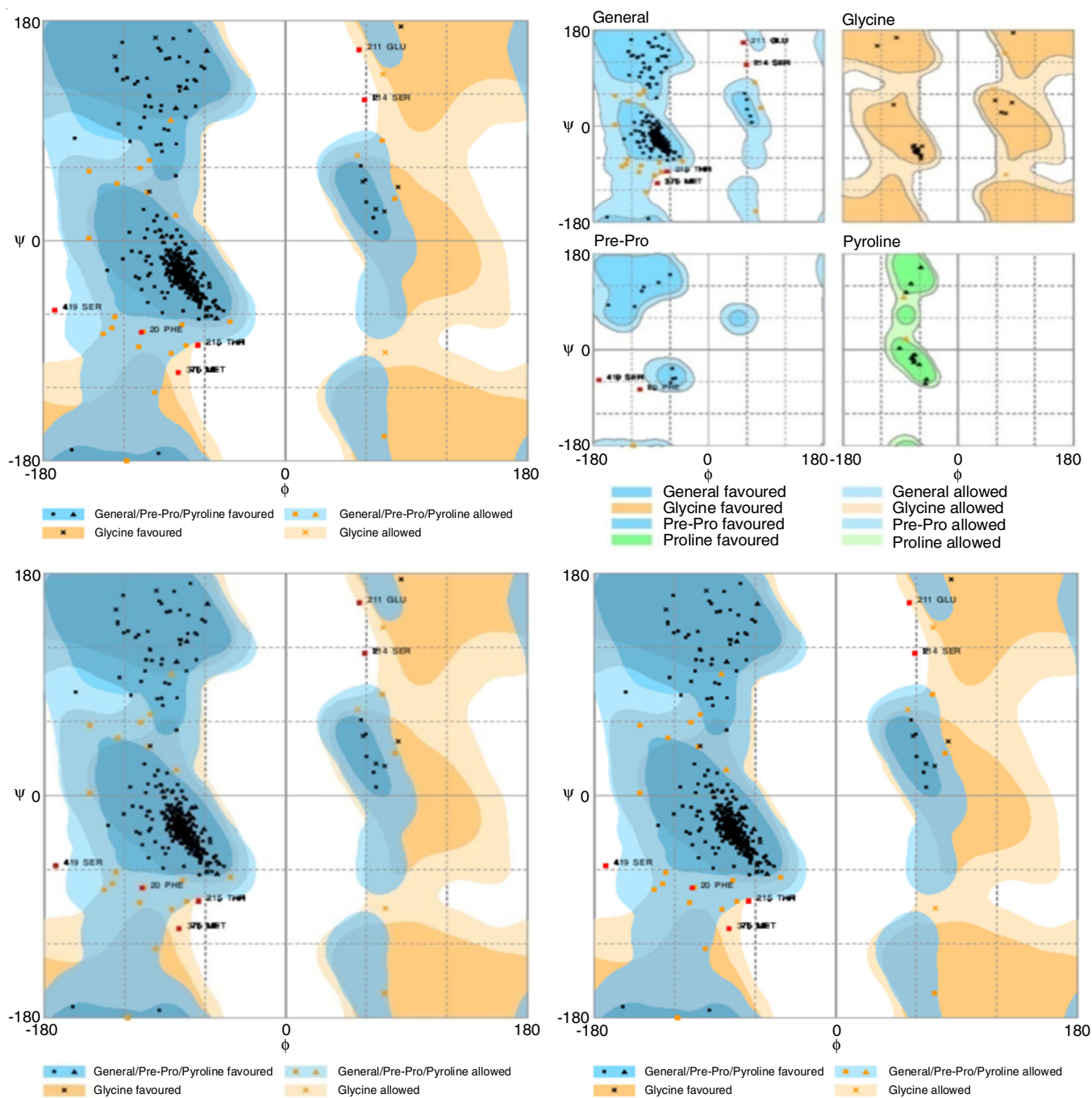


Fig. 4. Ramachandran plot of NADPH ubiquinone oxido reductase

TABLE-5  
SOSUI SERVER PREDICTION OF TRANSMEMBRANE REGION OF NADH-UBIQUINONE OXIDOREDUCTASE

| N terminal | Transmembrane region    | C terminal | Type      | Length |
|------------|-------------------------|------------|-----------|--------|
| 3          | LNIVFLPLLGSIIAGFFGGFIGA | 25         | PRIMARY   | 23     |
| 30         | FITVFCVGLTFCLSCLSFYEVGL | 52         | PRIMARY   | 23     |
| 75         | AFCFDSLTVVMLIVVTFISTLVH | 97         | PRIMARY   | 23     |
| 111        | PRFVSYLSLFTFFMLLVTADNF  | 133        | PRIMARY   | 23     |
| 136        | MFVWEGVGLCSYLLINFWFTRI  | 158        | SECONDARY | 23     |
| 176        | FGLALGIFTIFICFGAVDYATVF | 198        | PRIMARY   | 23     |
| 208        | TLNFLNIKFGALDLIGVLLFIGA | 230        | PRIMARY   | 23     |

Protein assays have shown that NADH-dependent oxidoreductase is the primary cause of nanoparticle formation. Reductase oxidizes NADH to NAD<sup>+</sup>, increasing the capacity to destroy metal ions. The analyzed results indicate that the *in silico* methods were designed to compare the similarity of the observed sequence of NADH quinone oxidoreductase. The resulting phylogenetic tree shows the distant relationship of *T. ornata* with *Asimina triloba* (above 90%), while remaining others are closely related to *Uvaria zeylanica*, *Meiogyne stenopetala*, etc.

The Ramachandran plot (Fig. 4) analyses revealed that the CPH model has 98% of the residues are in favoured region, 2% of the residues are in allowed region and 1.4% of residues are in outlier location. Pattern similarities and phylogenetic analysis of different plant species showed that the pattern found in *T. ornata* was identical. Hence, such plants like *T. ornata* are plentiful and can be used to synthesize nanoparticles and therapeutic agents.

## Conclusion

In this work, silver nanoparticles were synthesized by using bioreduction process with hydroalcoholic extract of seaweed *Turbinaria ornata*. The current synthetic method is found to be inexpensive and likely biocompatible due to the non-usage of any harsh or toxic components during the synthetic process. The UV and FTIR analyses were used to validate the conjugation and biomolecules involved in the reduction phase of silver nanoparticles obtained from *Turbinaria ornata*. Furthermore, the findings affirmed the efficacy of silver nanoparticles as antithrombolytic (71%) and anihemolytic (69%) agents. *in silico* Techniques were used to investigate the modifications and structural changes in proteins caused by the interaction with silver nanoparticles. The experimental results of silver nanoparticles synthesized from *T. ornata* were supported by the primary, secondary, and tertiary structures, as well as the Ramachandran plot of NADPH. Furthermore, it is possible to design drug delivery mechanisms which can provide significant preventive activity in the treatment of cardiac arrest and other associated diseases.

## CONFLICT OF INTEREST

The authors declare that there is no conflict of interests regarding the publication of this article.

## REFERENCES

- Miscellany, *Eur. J. Phycol.*, **42**(sup1), 23 (2007); <https://doi.org/10.1080/09670260701440760>
- J.K. Patra, G. Das, L.F. Fraceto, E. Campos, M. Rodriguez-Torres, L.S. Acosta-Torres, L.A. Diaz-Torres, R. Grillo, M.K. Swamy, S. Sharma, S. Habtemariam and H.S. Shin, *J. Nanobiotechnology*, **16**, 71 (2018); <https://doi.org/10.1186/s12951-018-0392-8>
- K.A. Leiss, Y.H. Choi, R. Verpoorte and P.G.L. Klinkhamer, *Phytochem. Rev.*, **10**, 205 (2010); <https://doi.org/10.1007/s11101-010-9175-z>
- N. Tyagi and S.S. Kumar, *Int. J. Res. Dev. Pharm. Life Sci.*, **6**, 7 (2017).
- P. Deepak, R. Sowmiya, G. Balasubramani and P. Perumal, *J. Taibah Univ. Med. Sci.*, **12**, 329 (2017); <https://doi.org/10.1016/j.jtumed.2017.02.002>
- K. Chakraborty, N.K. Praveen, K.K. Vijayan and G.S. Rao, *Asian Pac. J. Trop. Biomed.*, **3**, 8 (2013); [https://doi.org/10.1016/S2221-1691\(13\)60016-7](https://doi.org/10.1016/S2221-1691(13)60016-7)
- S.S. Dakshayani, M.B. Marulasiddeshwara, M.N.S. Kumar, G. Ramesh, P.R. Kumar, S. Devaraja and R. Hosamani, *Int. J. Biol. Macromol.*, **131**, 787 (2019); <https://doi.org/10.1016/j.ijbiomac.2019.01.222>
- R.N. Krishnaraj and R.N. Berchmans, *RSC Adv.*, **3**, 8953 (2013); <https://doi.org/10.1039/C3RA41246F>
- P. Mohanpuria, N. Rana and S.K. Yadav, *J. Nanopart. Res.*, **10**, 507 (2008); <https://doi.org/10.1007/s11051-007-9275-x>
- S. Shrivastava, T. Bera, S.K. Singh, G. Singh, P. Ramachandrarao and D. Dash, *ACS Nano*, **3**, 1357 (2009); <https://doi.org/10.1021/nn900277t>
- N.K. Hante, C. Medina and M.J. Santos-Martinez, *Front. Cardiovasc. Med.*, **6**, 139 (2019); <https://doi.org/10.3389/fcvm.2019.00139>
- B. Aslam, W. Wang, M.I. Arshad, M. Khurshid, S. Muzammil, M.H. Rasool, M.A. Nisar, R.F. Alvi, M.A. Aslam, M.U. Qamar, M.K.F. Salamat and Z. Baloch, *Infect. Drug Resist.*, **11**, 1645 (2018); <https://doi.org/10.2147/IDR.S173867>
- N. Karaki, C. Sebaaly, N. Chahine, T. Faour, A. Zinchenko, S. Rachid and H. Kanaan, *J. Appl. Pharm. Sci.*, **3**, 43 (2013); <https://doi.org/10.7324/JAPS.2013.30208>
- J. Laloy, V. Minet, L. Alpan, F. Mullier, S. Beken, O. Toussaint, S. Lucas and J.-M. Dogné, *Nanomedicines*, **1**, 1 (2014); <https://doi.org/10.5772/59346>
- A. Lateef, M.A. Akande, S.A. Ojo, B.I. Folarin, E.B. Gueguim-Kana and L.S. Beukes, *3 Biotech*, **6**, 140 (2016); <https://doi.org/10.1007/s13205-016-0459-x>
- A. Gabizon, D. Goren, R. Cohen and Y. Barenholz, *J. Control. Rel.*, **30**, 53 (1998); [https://doi.org/10.1016/s0168-3659\(97\)00261-7](https://doi.org/10.1016/s0168-3659(97)00261-7)
- K.P. Kumar, W. Paul and C.P. Sharma, *J. Bionanosci.*, **2**, 144 (2012); <https://doi.org/10.1007/s12668-012-0044-7>
- N.A.N. Mohamad, N.A. Arham, J. Junaidah, A. Hadi and S.A. Idris, *IOP Conf. Series: Mater. Sci. Eng. C.*, **358**, 012063 (2017); <https://doi.org/10.1088/1757-899X/358/1/012063>
- P. Deepak, R. Sowmiya, R. Ramkumar, G. Balasubramani, D. Aiswarya and P. Perumal, *Artificial Cells, Int. J. Nanomed.*, **45**, 990 (2016); <https://doi.org/10.1080/21691401.2016.1198365>
- S. Prasad, R.S. Kashyap, J.Y. Deopujari, H.J. Purohit, G.M. Taori and H.F. Dagainawala, *Thromb. J.*, **4**, 14 (2006); <https://doi.org/10.1186/1477-9560-4-14>
- E. Jun, K. Lim, K. Kim, O. Bae, J. Noh, K. Chung and J.-H. Chung, *Nanotoxicology*, **5**, 157 (2011); <https://doi.org/10.3109/17435390.2010.506250>

22. N.N. Hussein, *Biochem. Cell. Arch.*, **18**, 1721 (2019).
23. S.R. Vijayan, P. Santhiyagu, M. Singamuthu, N.K. Ahila, R. Jayaraman and K. Ethiraj, *Sci. World J.*, **2014**, 938272 (2014); <https://doi.org/10.1155/2014/938272>
24. S. Pirtarighat, M. Ghannadnia and S. Baghshahi, *J. Nanostruct. Chem.*, **9**, 1 (2019); <https://doi.org/10.1007/s40097-018-0291-4>
25. R.R.R. Kannan, W.A. Stirik and J. Staden, *S. Afr. J. Bot.*, **86**, 1 (2013); <https://doi.org/10.1016/j.sajb.2013.01.003>
26. A.M. Awwad, N.M. Salem and A.O. Abdeen, *Int. J. Ind. Chem.*, **4**, 29 (2013).
27. M.A. da Silva, M.F. Rossato, G. Trevisan, C.I.B. Walker, C.A.M. Leal, D.O. Borges, M.R.C. Schetinger, R.N. Moresco, M.M.M.F. Duarte, A.R.S. dos Santos, P.R.N. Viecili and J. Ferreira, *J. Evid. Based Complemen. Alternat. Med.*, **2012**, 954748 (2011); <https://doi.org/10.1155/2012/954748>
28. S. Audomkasok, W. Singpha, S. Chachiyo and V. Somsak, *J. Pathogens*, **2014**, 203154 (2014); <https://doi.org/10.1155/2014/203154>
29. M. Khalili, M.A. Ebrahimzadeh and Y. Safdari, *Arh. Hig. Rada Toksikol.*, **65**, 399 (2014); <https://doi.org/10.2478/10004-1254-65-2014-2513>
30. A. Raja, S.M. Salique, P. Gajalakshmi and A. James, *Int. J. Pharm. Sci. Nanotechnol.*, **9**, 1 (2016); <https://doi.org/10.37285/ijpsn.2016.9.1.6>
31. P. Appaiah and P. Vasu, *J. Proteomics Bioinform.*, **9**, 11 (2016); <https://doi.org/10.4172/jpb.1000417>
32. N. Ravooru, S. Ganji, N. Sathyanarayanan and H.G. Nagendra, *Front. Genet.*, **5**, 8 (2014); <https://doi.org/10.3389/fgene.2014.00291>